

Two new species of *Garra* (Teleostei: Cyprinidae) from western Iran

Mazaher Zamani-Faradonbe*, Yazdan Keivany*,
Salar Dorafshan* and E Zhang**

Two new species of *Garra* are described from the Iranian Tigris River drainage. *Garra meymehensis*, new species, from the Meymeh River, is distinguished by having 13–16 circumpeduncular scales, 7½ branched dorsal-fin rays, and 33–37 total lateral line scales, predorsal midline, and belly covered by free, non-embedded scales, chest covered by embedded scales and dorsal-fin origin closer to snout tip than to caudal-fin base. *Garra tiam*, new species, from the Abshur River, a tributary of the Karun, is distinguished by having 30–33 total lateral line scales, 12–13 circumpeduncular scales, 9–11 scales along the predorsal midline and dorsal-fin origin closer to caudal-fin base than to snout tip. The new species are also distinguished by a minimum K2P distance of 5.0 % between *G. meymehensis* and *G. tiam*, and 3.8 % between *G. tiam* and *G. gymnothorax*.

Introduction

Cyprinids of the genus *Garra* are widespread in the Persian Gulf basin, including the Tigris and Euphrates drainages (Hamidan et al., 2014; Esmaeili et al., 2018). *Garra* species of the Persian Gulf basins are placed in two well-separated species groups, the *G. rufa* and the *G. variabilis* groups (Hamidan et al., 2014). While the species of the *G. variabilis* group were recently studied by Mousavi-Sabet et al. (2019), here we have a closer look at the species richness of the *Garra rufa* species group in the Tigris River drainage. Seven species of the *G. rufa* species group are known from the Tigris River drainage, namely: *Garra rufa*, *G. amirhosseini*, *G. gymnothorax*, and

G. elegans (Esmaeili et al., 2016) plus three species endemic to subterranean habitats (*G. lorestanensis*, *G. typhlops*, and *G. tashanensis*). In the Euphrates, only *G. rufa* and the subterranean *G. widdowsoni* are known (Trewavas, 1955). Three additional species (*G. ghorensis*, *G. jordanica*, and *G. turcica*) are found in waters adjacent to the Euphrates River drainage in the west and other two (*G. mondica*, *G. persica*) in the coastal rivers of the Persian Gulf basin in Iran (Hamidan et al., 2014; Sayyadzadeh et al., 2015; Esmaeili et al., 2016; Mousavi-Sabet et al., 2019). The *Garra* species of the adjacent areas in the United Arab Emirates and Oman had been revised recently by Kirchner et al. (2020).

During fieldwork in western Iran, we found *Garra* specimens to be present almost everywhere,

* Department of Natural Resources (Fisheries Division), Isfahan University of Technology, Isfahan, 84156-83111, Iran. E-mails: mazaher.zamani@na.iut.ac.ir, keivany@iut.ac.ir, sdorafshan@iut.ac.ir

** Institute of Hydrobiology, Chinese Academy of Sciences, Wuhan, 430072, China. E-mail: zhange@ihb.ac.cn

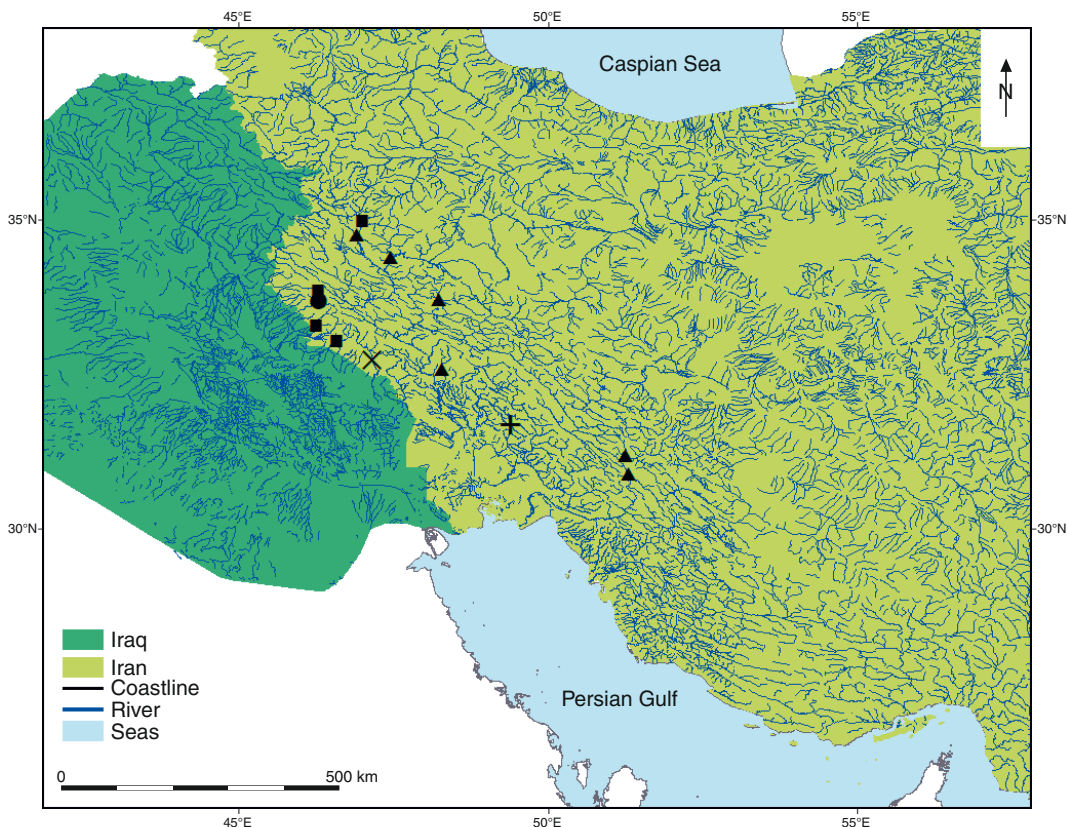


Fig. 1. Sampling sites of *Garra* specimens examined in this study. ●, *G. amirhosseini*; ▲, *G. gymnothorax*; ■, *G. rufa*; x, *Garra meymehensis*, new species (from Meymeh River); +, *Garra tiam*, new species (from Abshur River).

especially *G. rufa* and *G. gymnothorax* (Fig. 1). A detailed morphological study of these specimens in combination with DNA sequencing (COI) revealed two previously unknown molecular lineages that represent two new species, which are described and named further below.

Material and methods

After anaesthesia with 1 % clove oil solution, fishes were fixed and stored in 96 % ethanol. Measurements were made with a digital calliper and recorded to 0.1 mm. All measurements were made point to point. Methods for counts and measurements follow Kottelat & Freyhof (2007). The terminology of the snout morphology and the oromandibular structures follows Stiassny & Getahun (2007). We based the comparison of our new species on the specimens listed under Com-

parative material as well as on data published for *G. mondica* by Sayyadzadeh et al. (2015), *G. elegans* by Freyhof (2016), *G. typhlops* and *G. lorestanensis* by Mousavi-Sabet & Eagderi (2016), *G. persica* by Esmaeili et al. (2016), and *G. tashanensis* by Mousavi-Sabet et al. (2016). The map on Figure 1 is based on specimens examined during this study. Examined specimens belong to Isfahan University of Technology Ichthyology Museum, Iran (IUT-IM).

DNA extraction and PCR. Total cellular DNA was extracted from ethanol-preserved fin samples using CWBiotech Universal Genomic DNA kit following the manufacturer's instructions

Table 1. List of COI-sequences downloaded from NCBI > GenBank with information on drainage and country of origin.

Species	Drainage	Country	Accession number	Reference
<i>G. amirhosseini</i>	Tigris	Iran	KX570874	Esmaeili et al. (2016)
<i>G. amirhosseini</i>	Tigris	Iran	KM214780	Esmaeili et al. (2016)
<i>G. amirhosseini</i>	Tigris	Iran	KM214780	Hashemzadeh Segherloo et al. (2017)
<i>G. elegans</i>	Tigris	Iran	KM214702	Hamidan et al. (2014)
<i>G. elegans</i>	Tigris	Iraq	KM214721	Hamidan et al. (2014)
<i>G. gymnothorax</i>	Karun	Iran	KX570881	Esmaeili et al. (2016)
<i>G. gymnothorax</i>	Karun	Iran	KX570880	Esmaeili et al. (2016)
<i>G. gymnothorax</i>	Karun	Iran	KX570879	Esmaeili et al. (2016)
<i>G. gymnothorax</i>	Karun	Iran	KX570878	Esmaeili et al. (2016)
<i>G. gymnothorax</i>	Karun	Iran	KM214763	Esmaeili et al. (2016)
<i>G. gymnothorax</i>	Karun	Iran	KM214801	Esmaeili et al. (2016)
<i>G. gymnothorax</i>	Karun	Iran	KM214719	Esmaeili et al. (2016)
<i>G. gymnothorax</i>	Karun	Iran	KM214716	Esmaeili et al. (2016)
<i>G. gymnothorax</i>	Karun	Iran	KM214735	Esmaeili et al. (2016)
<i>G. gymnothorax</i>	Karun	Iran	KM373234	Esmaeili et al. (2016)
<i>G. gymnothorax</i>	Karun	Iran	MG852067	Hashemzadeh Segherloo et al. (2018)
<i>G. gymnothorax</i>	Karun	Iran	MG852066	Hashemzadeh Segherloo et al. (2018)
<i>G. lorestanensis</i>	Karun	Iran	MG852060	Hashemzadeh Segherloo et al. (2018)
<i>G. lorestanensis</i>	Karun	Iran	KM373228	Hashemzadeh Segherloo et al. (2017)
<i>G. lorestanensis</i>	Karun	Iran	KM214776	Hashemzadeh Segherloo et al. (2017)
<i>G. mondica</i>	Bushehr	Iran	MG852031	Hashemzadeh Segherloo et al. (2018)
<i>G. mondica</i>	Bushehr	Iran	MG852030	Hashemzadeh Segherloo et al. (2018)
<i>G. mondica</i>	Bushehr	Iran	KM214741	Esmaeili et al. (2016)
<i>G. mondica</i>	Bushehr	Iran	KM373226	Esmaeili et al. (2016)
<i>G. mondica</i>	Bushehr	Iran	KM214762	Esmaeili et al. (2016)
<i>G. persica</i>	Hurmoz	Iran	KM214807	Esmaeili et al. (2016)
<i>G. persica</i>	Hurmoz	Iran	KM214713	Esmaeili et al. (2016)
<i>G. persica</i>	Makran	Iran	KT808682	Esmaeili et al. (2016)
<i>G. persica</i>	Hurmoz	Iran	KM214747	Esmaeili et al. (2016)
<i>G. rufa</i>	Bushehr	Iran	KM214802	Hamidan et al. (2014)
<i>G. rufa</i>	Tigris	Iraq	KM214772	Hashemzadeh Segherloo et al. (2017)
<i>G. rufa</i>	Bushehr	Iran	KT808681	Sayyadzadeh et al. (2015)
<i>G. rufa</i>	Bushehr	Iran	KT808680	Sayyadzadeh et al. (2015)
<i>G. rufa</i>	Karun	Iran	JF416297	Hashemzadeh Segherloo et al. (2017)
<i>G. rufa</i>	Karun	Iran	KX570877	Esmaeili et al. (2016)
<i>G. rufa</i>	Karun	Iran	KX570876	Esmaeili et al. (2016)
<i>G. rufa</i>	Karun	Iran	KX570875	Esmaeili et al. (2016)
<i>G. rufa</i>	Bushehr	Iran	KM214810	Esmaeili et al. (2016)
<i>G. rufa</i>	Bushehr	Iran	KM214760	Esmaeili et al. (2016)
<i>G. rufa</i>	Tigris	Iran	KM214733	Esmaeili et al. (2016)
<i>G. rufa</i>	Maharlou	Iran	KM214714	Esmaeili et al. (2016)
<i>G. rufa</i>	Karun	Iran	KM214711	Esmaeili et al. (2016)
<i>G. rufa</i>	Zohreh	Iran	KM214709	Esmaeili et al. (2016)
<i>G. rufa</i>	Tigris	Iraq	KM214777	Hamidan et al. (2014)
<i>G. rufa</i>	Bushehr	Iran	KM214761	Esmaeili et al. (2016)
<i>G. rufa</i>	Bushehr	Iran	KM214754	Esmaeili et al. (2016)
<i>G. rufa</i>	Tigris	Iraq	KM214700	Hashemzadeh Segherloo et al. (2017)
<i>G. rufa</i>	Tigris	Iraq	KM214739	Esmaeili et al. (2016)
<i>G. tashanensis</i>	Jarrahi	Iran	KY365751	Mousavi-Sabet et al. (2016)
<i>G. tashanensis</i>	Jarrahi	Iran	KY365750	Mousavi-Sabet et al. (2016)
<i>G. typhlops</i>	Karun	Iran	MG852061	Hashemzadeh Segherloo et al. (2018)
<i>G. typhlops</i>	Karun	Iran	KM214731	Hamidan et al. (2014)
<i>G. typhlops</i>	Karun	Iran	JF416299	Hashemzadeh Segherloo et al. (2012)
<i>G. typhlops</i>	Karun	Iran	MG852034	Hashemzadeh Segherloo et al. (2018)
<i>G. widdowsoni</i>	Tigris	Iraq	KM214795	Hamidan et al. (2014)
<i>G. widdowsoni</i>	Tigris	Iraq	KM214769	Hamidan et al. (2014)

(tissue protocol) and in some samples, extracted employing ammonium acetate salt method suggested by Bruford et al. (1998). The COI gene was amplified using primers FCOI20 (5'-AACCTCTGTCTTCGGGGCTA-3') and RCOI20 (5'-AGTGGTTATGYGGCTGGCTT-3') (Hashemzadeh Segherloo et al., 2012). Polymerase chain reaction (PCR) condition was as follows: a 25 µl final reaction volume containing 2.5 µl of 10 X Taq polymerase buffer, 0.75 µl of (50 mM) MgCl₂, 0.5 µl of (10 mM) dNTPs, 0.75 µl (10 mM) of each primer, 0.5 µl of Taq polymerase (5 U µl⁻¹), 3.5 µl of total extracted DNA, and 15.75 µl of distilled H₂O. Amplification cycles were as follows: denaturation for 10 min at 94 °C; 35 cycles at 94 °C for 1 min, 62–63 °C for 1 min, 72 °C for 1 min and a final extension for 10 min at 72 °C, and sequencing was completed by Tianyihuiyuan Biotechnology Company using the amplification primer.

Molecular data analysis. COI sequences (DNA barcodes) were generated from 60 individuals of *Garra* from Iran. Additionally, we included 56 sequences already published on NCBI GenBank (Table 1). Data processing and new sequence alignment were carried out in MEGA7 software (Kumar et al., 2016) based on ClustalW algorithm (Higgins & Sharp, 1988). COI gene sequences from a total of 116 samples of *Garra* were included in this study. The nucleotide substitution pattern calculated with DAMBE v. 6 (Xia, 2013, 2017) showed that the sequences have not reached substitution saturation; the software Partition-Finder v. 2 (Lanfear et al., 2016) was employed to determine the best fit substitution model (codon position 1/2/3 = TRN+I+G \ TVM+I \ TRN+G).

Bayesian analyses of nucleotide sequences were run with the MrBayes 3.1.2 (Ronquist et al., 2012) to examine the optimal tree topology. Here, Bayesian analyses were performed using four MCMC chains of 10⁷ generations each to estimate the posterior probability distribution at the default temperature (0.2). Topologies were sampled every 1000 generations. Maximum likelihood phylogenetic trees were generated with 10000 bootstrap replicates in RAxML v8.2.X software (Stamatakis, 2014) under the GTR+G+I model of nucleotide substitution. The results were visualised with FigTree v. 1.4.

Estimates of evolutionary divergence (genetic distances) over sequence pairs between species were conducted in MEGA7 software (Kumar et al., 2016) using the Kimura 2-parameter model (Kimura, 1980), the rate variation among sites was modelled with a gamma distribution (shape parameter = 1), codon positions included were 1st + 2nd + 3rd + noncoding. All positions containing gaps and missing data were used. As out-group, *Cyprinus carpio* from GenBank (accession number: KC789529) was used in COI phylogenetic analysis.

To delimit species, the Poisson tree process (PTP) model, using a distance-based tree implemented in Bayesian PTP (bPTP; Zhang et al., 2013), was used. This analysis was performed using the online server of Exelixis Labs (<http://species.h-its.org/ptp>) (accessed 9 November 2019). The analyses were run for 10000 generations with a thinning of 100 and burn-in of 0.1. Visualizing plots of MCMC iteration vs. log-likelihood were used to assess the convergence.

Table 2. Estimates of the average evolutionary divergences among *Garra* species.

	1	2	3	4	5	6	7	8	9	10	11
1 <i>G. amirhosseini</i>											
2 <i>G. elegans</i>	0.6										
3 <i>G. gymnothorax</i>	6.8	6.1									
4 <i>G. lorestanensis</i>	7.0	6.7	4.2								
5 <i>G. meymehensis</i>	8.5	8.2	5.2	5.4							
6 <i>G. mondica</i>	2.0	1.5	5.7	6.5	8.0						
7 <i>G. persica</i>	4.4	4.7	6.2	4.9	6.4	4.4					
8 <i>G. rufa</i>	4.7	4.5	6.1	4.8	5.7	4.2	2.5				
9 <i>G. tashanensis</i>	10.3	10.6	12.5	10.6	12.3	9.8	9.4	9.9			
10 <i>G. tiam</i>	8.4	8.1	3.8	4.8	5.0	8.3	7.6	7.3	12.2		
11 <i>G. typhlops</i>	7.5	7.7	4.8	3.8	5.1	7.9	5.5	5.9	11.5	4.8	
12 <i>G. widdowsoni</i>	4.7	4.4	7.0	5.7	8.2	4.5	3.7	3.2	10.9	8.1	7.6

Fig. 2. Phylogenetic tree of mitochondrial COI barcode region based on Maximum Likelihood (ML). Numbers on branches indicate Maximum Likelihood (ML) bootstrap and posterior probability values for Bayesian inference (ML \ BI). Black solid bars right to the specimen labels indicate species delimitation results from Bayesian Poisson tree process (bPTP).



Results

Phylogenetic analysis and sequence variation.

Bayesian inference estimation of phylogenetic relationships and species delimitation methodology based on mitochondrial COI barcode region recovered 12 lineages (Fig. 2), including a clade for specimens of *Garra* from Meymeh River, and a clade for specimens of *Garra* from Abshur River. These two together with *G. gymnothorax* were grouped in a more inclusive clade. The species delimitation methodology used in this study (bPTP) supported the recognition of these two lineages (from Meymeh River and Abshur River), as two distinct species. The average evolutionary divergences in the mtDNA COI barcode region among *Garra* species is shown in Table 2. The phylogenetic tree recovered the species of the *G. rufa* species-group split in three main clades: Clade I: *G. gymnothorax*, *Garra* sp. 1 (from Meymeh River), *Garra* sp. 2 (from Abshur River), *G. typhlops*, and

G. lorestanensis; Clade II: *G. rufa*, *G. amirhosseini*, *G. elegans*, *G. mondica*, *G. widdowsoni*, and *G. persica*; and Clade III: *G. tashanensis* specimens.

Based on these results, the specimens from Meymeh River (*Garra* sp. 1) and Abshur River (*Garra* sp. 2) are recognized as representatives of two new species, described and named further below as *G. meymehensis* and *G. tiam*.

Garra meymehensis, new species (Figs. 3–9)

Holotype. IUT-IM M43, 49.0 mm SL; Iran: Ilam Prov.: Meymeh River at km 16 on road from Dehloran to Mehran, 32°44'33"N 47°9'23"E; M. Zamani-Faradonbe and H. Khoshnamvand, 2 Nov 2017.

Paratypes. IUT-IM 13981019-01-01, 57, 33.7–71.4 mm SL; collected with the holotype.

Table 3. Morphometric data of *Garra meymehensis*. Holotype, IUT-IM M43; paratypes, IUT-IM 13981019-01-01 (n=57). Size range includes the holotype. SD, standard deviation.

	Holotype	range	mean	SD
Standard length	49.0	33.7–71.4	44.8	–
In percent of standard length				
Head length	23.9	23.3–28.7	25.6	1.5
Body depth at dorsal-fin origin	24.0	18.6–30.6	24.2	2.5
Predorsal length	49.1	29.8–53.2	48.8	4.2
Postdorsal length	32.2	25.7–42.5	34.0	3.1
Preanal length	77.9	75.2–86.3	80.2	2.6
Prepectoral length	22.0	20.8–26.8	23.9	1.3
Prepelvic length	56.0	45.7–61.3	56.5	2.9
Distance between pectoral and pelvic-fin insertions	34.1	28.5–40.1	34.7	2.8
Distance between pectoral-fin insertion and anal-fin origin	56.0	40.6–64.9	57.5	4.5
Distance between pelvic-fin insertion and anal-fin origin	22.2	19.5–27.7	24.1	2.0
Depth of caudal peduncle	12.0	11.4–14.6	12.8	0.8
Length of caudal peduncle	10.6	7.0–18.3	13.8	2.0
Dorsal fin height	22.1	18.7–25.5	22.7	1.7
Dorsal fin base length	18.3	14.3–20.1	16.5	1.3
Anal fin-base length	9.4	6.6–10.4	8.8	0.9
Pectoral-fin length	24.0	14.8–26.5	19.5	2.6
Pelvic-fin length	18.3	12.7–25.3	16.6	2.3
In percent of head length				
Head depth	70	57–75	65.0	4.0
Snout length	35	35–61	43.2	5.5
Postorbital distance	40	32–80	42.4	3.1
Interorbital width	55	50–70	60.5	4.0
Eye diameter	25	19–28	23.6	2.3
Maximum head width	70	68–90	76.3	4.5
Internostril width	34	29–60	37.5	4.6

Material for molecular genetic analysis (non-types). IUT-IM M43a, M43, M44, M45, M46, M115; same data as holotype (GenBank accession numbers: MN255038–MN255043).

Diagnosis. *Garra meymehensis* is distinguished from other species of *Garra* in the Persian Gulf basin by a combination of characters, none of them unique to the species. It is distinguished from *G. amirhosseini* by having exposed non-embedded scales on the belly and predorsal midline (vs. embedded). It is distinguished from *G. gymnothorax* and *G. rufa* by having usually $7\frac{1}{2}$ branched dorsal-fin rays (vs. $8\frac{1}{2}$). The chest of *Garra meymehensis* is covered by embedded scales while its belly exhibits exposed non-embedded scales. The scale pattern of the chest and belly is very variable in *G. gymnothorax* and *G. rufa*. While a scaleless chest is regularly found in *G. gymnothorax*, it is rare in *G. rufa*, whose chest is usually covered by exposed or embedded scales. *Garra meymehensis* is distinguished from *G. persica* by having $9+8$ caudal-fin rays (vs. $8+8$) and from *G. mondica* by having the chest covered by embedded scales and belly with free, non-embedded scales (vs. chest and belly scaleless or with very small scales deeply embedded), and 6–7 (usually 6) scales from the base of the last pelvic-fin ray to the anterior margin of the anus (vs. 4–6, usually 5). *Garra meymehensis* is distinguished from subterranean *Garra* species from the Iranian Tigris River drainage by having the flank fully covered by scales (vs. scaleless in *G. lorestanensis* and *G. typhlops*, and few scales on anterior part of flank in *G. tashanensis*), a well-developed mental disc (vs. absent in *G. typhlops*), a well-developed eye (vs. reduced in *G. lorestanensis*, *G. tashanensis*, and *G. typhlops*), and a pigmented body surface (vs. no pigmentation in *G. lorestanensis*, *G. typhlops*, and *G. tashanensis*). *Garra meymehensis* is distinguished from *G. elegans* by having free lateral and posterior margins of the mental disc (vs. fully attached).

Description. See Figures 3 to 9 for general appearance and Table 3 for morphometric data of holotype and paratypes. Small-sized and elongated species with relatively shallow caudal peduncle. Dorsal head profile rising gently from tip of snout to nape, dorsal profile of back slightly convex from nape to dorsal-fin origin. Ventral profile more or less straight between pectoral-fin insertion and anal-fin origin. Body deepest at or slightly in front

of dorsal-fin base and body depth decreasing towards caudal-fin base. Greatest body width at or slightly behind of pectoral-fin base. Body almost equally wide from pectoral-fin base to dorsal-fin origin. Head moderately large (23.3–28.7 % SL) and slightly depressed (57–73 % HL). Interorbital space slightly convex or flat, height at nape less than head length. Head length 0.8–1.4 times in body depth. Snout rounded, its length 0.6–1.5 times in postorbital length. No obvious tubercle on transverse lobe; demarcated posteriorly by a shallow transverse groove in some specimens. Small- or medium-sized tubercles sparsely set on proboscis, larger on its anterior margin. Small- to medium-sized tubercles scattered through lateral and dorsal surface of snout reaching posterior nostril in most specimens, or anterior orbital margin in a few. Depressed rostral surface always lacking tubercles; transverse lobe moderately separated from lateral surface in large specimens. Anterior arm of depressed rostral surface not reaching to base of rostral barbel. No groove between transverse lobe and lateral surface in some individuals.

Eye relatively large, its diameter 0.25–0.50 times in head depth and 0.25–0.46 times in interorbital width. Two pairs of barbels, maxillary barbel at corner of mouth, shorter (0.7–0.8 times) than rostral barbel, rostral barbel anterolaterally located, shorter (0.7–0.9 times) than eye diameter. Rostral cap well-developed, fimbriate, papillate on ventral surface. Upper lip present as a thin band of papillae arranged in one or two ridges. Upper jaw almost or completely covered by rostral cap. Disc almost oval in shape, longer than wide, and narrower than head width through base of maxillary barbel. Papillae on anterior fold equally-sized and regularly arranged. Narrow and deep groove between anteromedial fold and central callous pad (shallow in some individuals); scattered small-sized papillae on latero-posterior flap. Surface of central callous pad without or with sparsely arranged small papillae.

Dorsal fin with 2–3 simple and $7\frac{1}{2}$ – $8\frac{1}{2}$ [$7\frac{1}{2}$ (55), $8\frac{1}{2}$ (3)] branched rays, last simple ray shorter than head length, distal margin slightly concave, origin closer to snout-tip than to caudal-fin base, first branched ray longest, tip of last branched ray reaching vertical to, or slightly in front of anus when folded down. Pectoral fin with one simple and 10–13 [10 (3), 11 (44), 12 (3), 13 (8)] branched rays. Tip of pectoral fin approximately reaching a point 3–4 scales anterior to pelvic-fin insertion; its length shorter than head length. Pelvic fin with

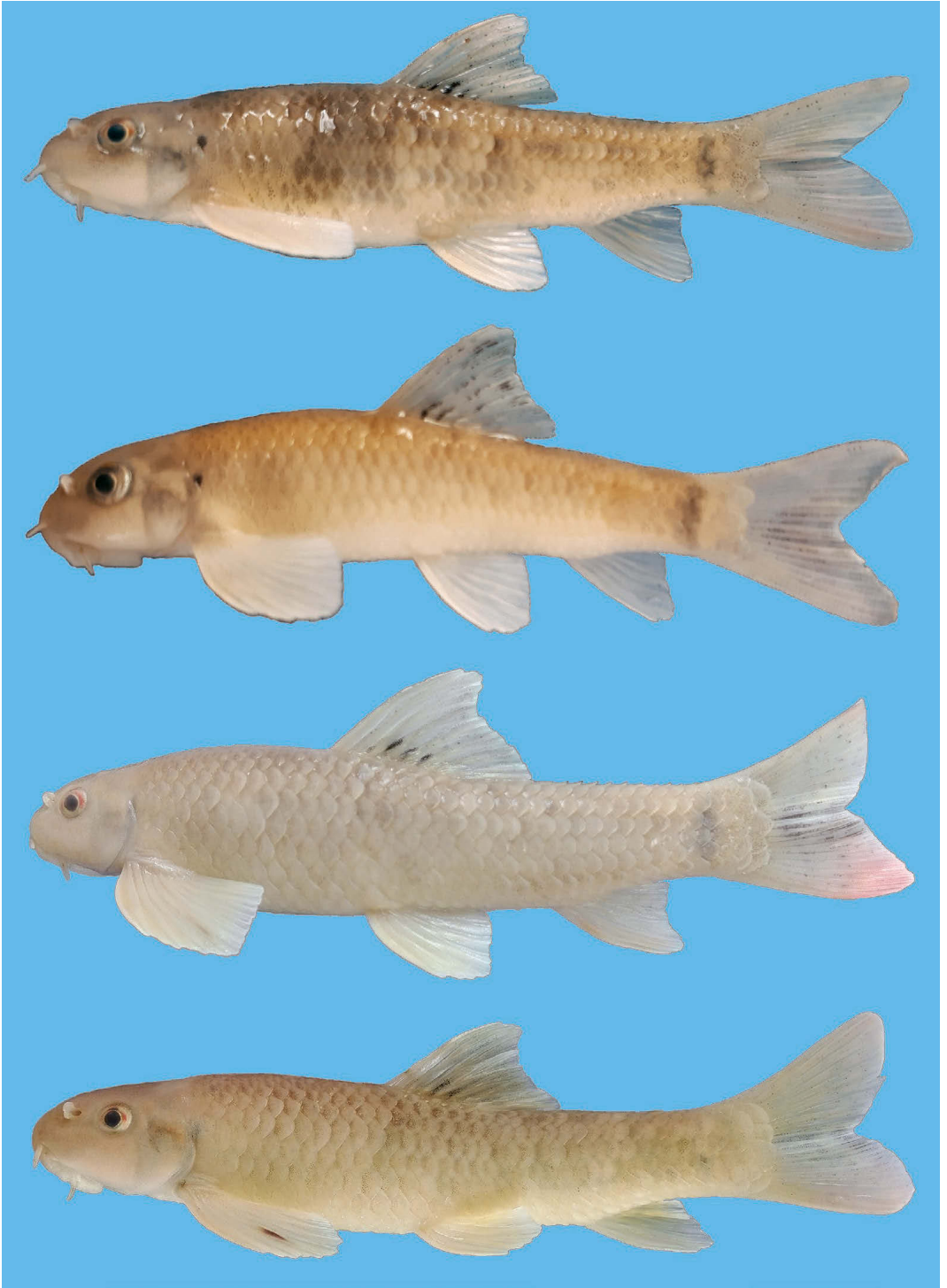


Fig. 3. *Garra meymehensis*, from top to bottom, IUT-IM M43, holotype, 49.0 mm SL; IUT-IM 13981019-01-01, para-types, 43.1 mm SL, 67.1 mm SL, 71.4 mm SL; Iran: Meymeh River.



Fig. 4. *Garra meymehensis*, from top to bottom, IUT-IM M43, holotype, 49.0 mm SL; IUT-IM 13981019-01-01, para-
types, 43.1 mm SL, 67.1 mm SL, 71.4 mm SL; Iran: Meymeh River.

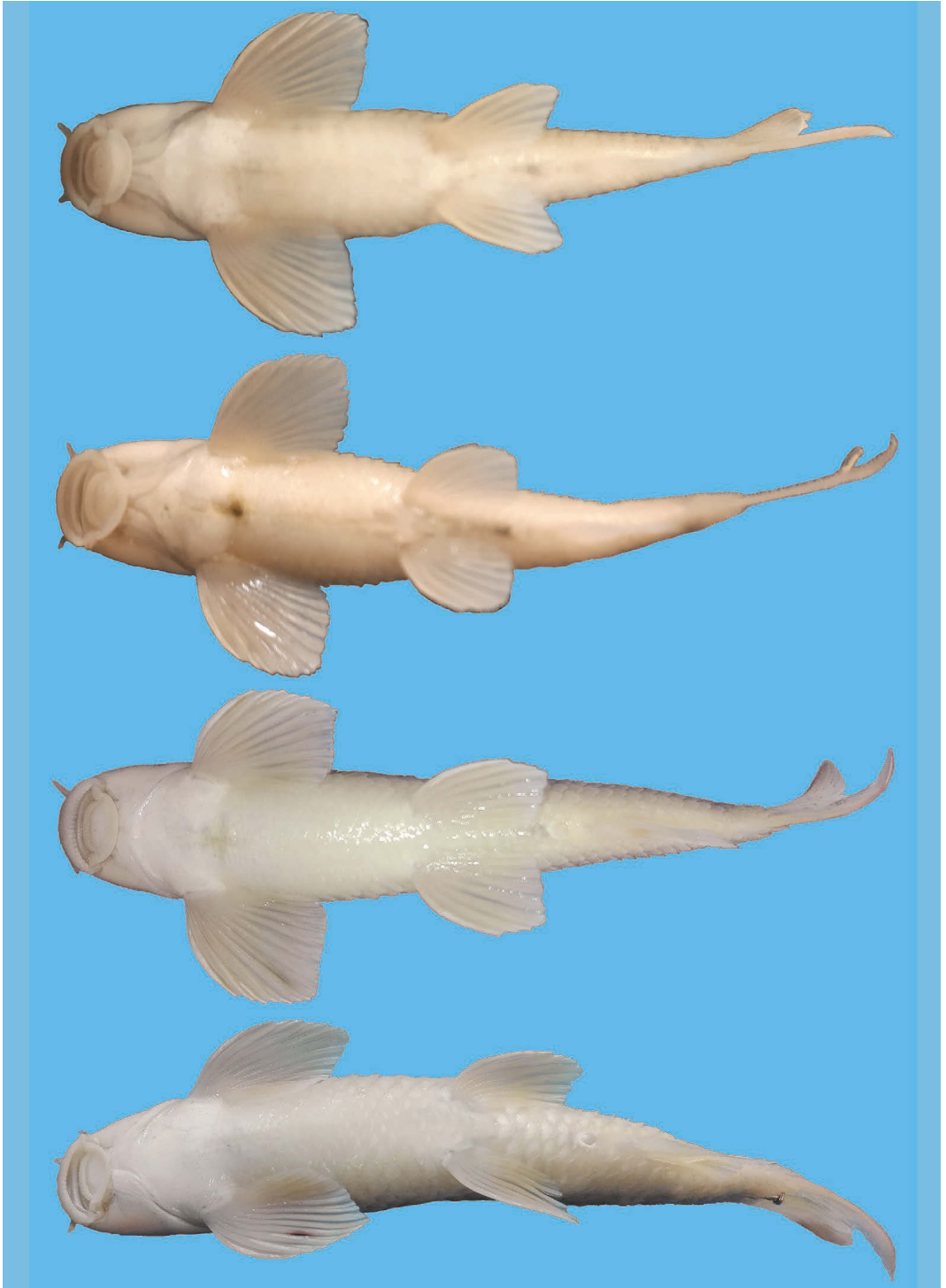


Fig. 5. *Garra meymehensis*, from top to bottom, IUT-IM M43, holotype, 49.0 mm SL; IUT-IM 13981019-01-01, para-
types, 43.1 mm SL, 67.1 mm SL, 71.4 mm SL; Iran: Meymeh River.



Fig. 6. *Garra meymehensis*, from left to right, IUT-IM M43, holotype, 49.0 mm SL; IUT-IM 13981019-01-01, paratypes, 43.1 mm SL, 67.1 mm SL, 71.4 mm SL; Iran: Meymeh River.



Fig. 7. *Garra meymehensis*, from left to right, IUT-IM M43, holotype, 49.0 mm SL; IUT-IM 13981019-01-01, paratypes, 43.1 mm SL, 67.1 mm SL, 71.4 mm SL; Iran: Meymeh River.



Fig. 8. *Garra meymehensis*, from left to right, IUT-IM M43, holotype, 49.0 mm SL; IUT-IM 13981019-01-01, paratypes, 43.1 mm SL, 67.1 mm SL, 71.4 mm SL; Iran: Meymeh River.

one simple and 6–7 [6(3), 7(55)] branched rays; its tip not reaching to anus or anterior margin of anal-fin base. Insertion of pelvic fin closer to anal-fin origin than to pectoral-fin insertion. Anal fin

short, with 2 simple and 5½ branched rays, first branched ray longest, distal margin straight or slightly concave, origin closer to caudal-fin base than to pelvic-fin insertion in most specimens.



Fig. 9. *Garra meymehensis*, live coloration, IUT-IM 13981019-01-01, paratype, 43.1 mm SL; Iran: Meymeh River.

Anus 2–3 [2(4), 3(16)] scales distant from anal-fin origin. Caudal peduncle length 0.8–1.5 times longer than its depth. Caudal fin distinctly forked with 9+8 branched rays [except 9+7(1), 9+9(2)]; tip of caudal lobes pointed. Total gill rakers on first branchial arch 16–20 [16(2), 17(4), 18(6), 19(2), 21(1)]. Lateral line complete, totally with 33–37 [33(10), 34(29), 35(15), 36(3), 37(1)] scales, 2–3 scales on caudal-fin base. Transverse scale rows above lateral line 3–5 [3(2), 4(50), 5(6)]. Scale rows between lateral line and pelvic-fin insertion 3–4 [3(15), 4(43)] and between lateral line and anal-fin origin 3–4 [3(34), 4(24)]. Circumpeduncular scale rows 13–16 [13(1), 14(12), 15(27), 16(18)]. Eleven non-embedded exposed scales along predorsal midline of 48 specimens examined. Ten specimens bearing slightly or deeply embedded scales on predorsal midline. Scales regularly set on flanks. Chest covered by embedded scales. Scales on belly with free margins, exposed, not embedded in skin. Chest and belly scaleless in eight out of 58 specimens; and 6–7 [6(14), 7(6)] scales between tip of pelvic fin and anus.

Coloration. In ethanol: dorsal surface of head, dorsum and flank pale brown. Single or patches of dark-brown scales on the flanks. Ventral surface of head, mouth, chest and abdomen whitish yel-

low. A large, 2–3 scales wide, black bar on distal portion of caudal peduncle, very conspicuous in most specimens, faded in a few. A black blotch at anteriormost lateral line. Pectoral, pelvic and anal fins light grey to yellow. Some black to dark-brown blotches on caudal-fin membranes. Dorsal-fin membranes with a black or dark-grey blotch at base, some black or brown blotches on middle and distal dorsal-fin membranes.

In life: background colour bright silvery to pale green. Fins hyaline, paired fins golden yellow with black dots. Head grey to green. Iris silvery orange; dark brown spot at upper portion. Scales on flanks silvery green and dark grey, whitish or pale grey on ventral part of flank and belly, rostral barbel with small black dots.

Distribution. *Garra meymehensis* is currently known from the Meymeh River, a tributary of the lower Tigris River. Meymeh River is located in Ilam Province of Iran, with a length of 145 km in Iranian territory. Meymeh River is a perennial river. In Iraq, its name changes to Nahre-Al-Tayeb and then near the Al-Amarah city it flows into the Tigris.

Etymology. *Meymehensis*, -is, -e, referring to Meymeh River. An adjective.

Garra tiam, new species
(Figs. 10–16)

Holotype. IUT-IM T43, 62.8 mm SL; Iran: Khozestan Prov.: Abshur River at km 40 on the road from Masjed Soleyman to Haftgel, 31°41'33"N 49°24'17"E; M. Zamani-Faradonbe and H. Khoshnamvand, 2 Nov 2017.

Paratypes. IUT-IM 13981018-01-01, 26, 29.0–70.8 mm SL; collected with the holotype.

Material for molecular genetic analysis (non types). IUT-IM T56–T58, T57a, T58a; same data as holotype (GenBank accession numbers: MN255044–MN255048).

Diagnosis. *Garra tiam* is distinguished from other species of *Garra* in the Persian Gulf basin by a combination of characters, none unique to the species. It is distinguished from *G. amirhosseini* by having usually 8½ branched dorsal-fin rays

(vs. usually 7½) and the number of circumpeduncular scales (12–13 vs. 13–14, respectively). *Garra tiam* is distinguished from *G. meymehensis* by having usually 8½ branched dorsal-fin rays (vs. usually 7½) and the number of scales on the lateral line (30–33 vs. 33–37, respectively). *Garra tiam* is distinguished from *G. gymnothorax* and *G. rufa* by having 30–33 total lateral line scales (vs. 32–37) and 12–13 circumpeduncular scales (vs. 13–17). It is distinguished from *G. persica* by having 9+8 branched caudal-fin rays (vs. 8+8) and 19–22 total gill rakers on the first branchial arch (vs. 17–19). *Garra tiam* is distinguished from *G. mondica* by having 8½ branched dorsal-fin rays (vs. 7½), the belly covered by scales (vs. scaleless). *Garra tiam* is distinguished from the subterranean *Garra* species from the Tigris River drainage by having the flanks fully covered by scales (vs. scaleless in *G. lorestanensis* and *G. typhlops*; or with few scales on anterior portion of flanks in *G. tashanensis*), a well-developed mental disc (vs. absent in *G. typhlops*), well-developed eye

Table 4. Morphometric data of *Garra tiam*, holotype, IUT-IM T43; paratypes, IUT-IM 13981018-01-01 (n=26). Size range includes the holotype. SD, standard deviation.

	Holotype	range	mean	SD
Standard length	62.8	29.0–70.8	49.7	10.8
In percent of standard length				
Head length	26.2	19.7–28.5	24.9	2.2
Body depth at dorsal-fin origin	24.8	19.7–31.5	25.6	2.9
Predorsal length	48.2	45.5–54.6	49.3	2.5
Postdorsal length	32.5	25.1–36.3	32.4	2.4
Preanal length	78.4	69.6–86.2	79.5	3.7
Prepectoral length	24.9	18.7–26.5	24.2	1.7
Prepelvic length	55.8	49.7–62.0	56.6	3.2
Distance between pectoral and pelvic-fin insertions	32.2	18.1–39.4	33.3	4.0
Distance between pectoral-fin insertion and anal-fin origin	58.5	51.4–88.5	58.6	6.6
Distance between pelvic-fin insertion and anal-fin origin	25.6	20.2–29.7	25.0	2.4
Depth of caudal peduncle	13.4	12.5–15.6	14.1	0.8
Length of caudal peduncle	13.4	9.3–16.5	12.7	1.6
Dorsal fin height	22.9	14.7–26.3	22.7	2.1
Dorsal fin base length	16.8	14.7–21.6	17.6	1.6
Anal fin-base length	8.6	7.3–10.1	8.7	0.8
Pectoral-fin length	24.4	12.2–24.9	20.9	3.2
Pelvic-fin length	20.8	15.0–22.1	19.4	1.9
In percent of head length				
Head depth	67	60–88	68.6	6.2
Snout length	47	36–62	43.7	5.1
Postorbital distance	32	29–51	38.4	5.3
Interorbital width	61	52–72	59.2	5.0
Eye diameter	20	19–33	25.7	3.7
Maximum head width	71	61–89	73.1	6.5
Internostril width	35	32–47	37.1	3.9

(vs. reduced in *G. lorestanensis*, *G. typhlops*, and *G. tashanensis*), and a pigmented body surface (vs. no pigmentation in *G. lorestanensis*, *G. typhlops*, and *G. tashanensis*). It is distinguished from *G. elegans* by having free lateral and posterior margins of the mental disc (vs. fully attached).

Description. See Figures 10 to 16 for general appearance and Table 4 for morphometric data of holotype and paratypes. Small-sized and elongated species with a shallow caudal peduncle. Dorsal head profile rising gently from the tip of snout to nape, dorsal profile of back slightly convex from nape to dorsal-fin origin. Ventral profile more or less straight between pectoral-fin insertion and anal-fin origin. Body deepest at or slightly in front of dorsal-fin base, body depth decreasing towards caudal-fin base. Greatest body width at or slightly behind pectoral-fin base, body almost equally between pectoral-fin base and dorsal-fin origin. Head moderately large [its length 19.7–28.5 % SL] and slightly depressed [its depth 60–88 % HL], with slightly convex or flat interorbital space, height at nape less than head length. Head length 0.8–1.4 times in body depth. Snout rounded, its length 0.6–1.6 times in postorbital length. Transverse lobe with tubercle, demarcated posteriorly by a shallow transverse groove in most specimens (groove sometimes absent). Medium- to large tubercles sparsely set on proboscis; largest on its anterior margin. Medium- to large sized tubercles scattered through lateral and dorsal surface of snout reaching anterior nostril in most specimens, or posterior orbital margin in a few specimens. Depressed rostral surface lacking tubercles; transverse lobe moderately separated from lateral surface; separation not conspicuous in some specimens. Anterior arm of depressed rostral surface not reaching to base of rostral barbel. No groove between transverse lobe and lateral surface in some individuals. No head tubercles in small individuals.

Eye relatively large, its diameter 0.3–0.4 times in head depth and 0.3–0.5 times in interorbital width. Two pairs of barbels, maxillary barbel at corner of mouth, shorter (0.4–0.5 times) than rostral barbel, rostral barbel anterolaterally located, shorter (0.6–0.7 times) than eye diameter. Rostral cap well-developed, fimbriate, papillate on ventral surface. Upper lip present, as a thin band of papillae arranged in some ridges. Upper jaw almost or completely covered by rostral cap. Mental disc almost round, longer than wide and

narrower than head width through maxillary barbel. Papillae on anterior fold of same size specimens regularly arranged. Groove between antero-medial fold and central callous pad narrow and deep, scattered small-sized papillae on latero-posterior flap; surface of central callous pad without or with sparsely arranged small papillae.

Dorsal fin with 2 simple and 8½ (26) branched rays, last simple ray shorter than head length, distal margin slightly concave, origin closer to caudal-fin base than to snout tip, first branched ray longest, tip of last branched ray reaching vertical to, or slightly in front of anus when folded down. Pectoral fin with one simple and 11–14 [11 (14), 12 (7), 13 (4), 14 (1)] branched rays, its tip approximately reaching a point 3–4 scales anterior to pelvic-fin insertion, its length shorter than head length. Pelvic fin with one simple and 6–8 [6 (4), 7 (18), 8 (4)] branched rays, its tip not reaching to anus or anterior margin of anal fin. Insertion of pelvic fin closer to anal-fin origin than to pectoral-fin insertion. Anal fin short, with 2 simple and 5½ branched rays, first branched ray longest, distal margin straight or slightly concave, origin closer to caudal-fin base than to pelvic-fin insertion. Anus 2–3 [2 (14), 3 (3)] scales distant from anal-fin origin. Caudal peduncle length 0.5–1.4 times longer than its depth. Caudal fin distinctly forked with 9+8 branched rays, tip of caudal lobes pointed. Total gill rakers on first branchial arch 18–22 [18 (3), 19 (3), 20 (5), 21 (4), 22 (1)]. Lateral line complete, totally with 30–34 [30 (3), 31 (4), 32 (10), 33 (5), 34 (4)] scales, 2–3 scales on caudal-fin base. Transverse scale rows above lateral line 3–4 [3 (14), 4 (12)]. Scale rows between lateral line and pelvic-fin insertion 3–4 [3 (23), 4 (3)] and between lateral line and anal-fin origin 3–4 [3 (22), 4 (4)]. Circumpeduncular scale rows 12–13 [12 (10), 13 (17)]. Eleven scales along predorsal midline in one specimen, nine scales with free posterior margins along predorsal midline in four specimens and embedded in others. Scales regularly set on flank. Chest scaleless and belly covered with scales with free posterior margins. Five or six [5 (14), 6 (3)] scales between posteriormost pelvic-fin base and anus.

Coloration. In ethanol: dorsal surface of head, dorsum and flank dark brown to black. Single or groups of dark-brown scales on flank. Ventral surface of head, mouth, chest and abdomen whitish yellow. A large, 2–3 scales wide, black or dark-brown blotch on distal portion of caudal



Fig. 10. *Garra tiam*, from top to bottom, IUT-IM T43, holotype, 62.8 mm SL; IUT-IM 13981018-01-01, paratypes, 44.7 mm SL, 54.2 mm SL, 68.1 mm SL; Iran: Abshur River.



Fig. 11. *Garra tiam*, from top to bottom, IUT-IM T43, holotype, 62.8 mm SL; IUT-IM 13981018-01-01, paratypes, 44.7 mm SL, 54.2 mm SL, 68.1 mm SL; Iran: Abshur River.

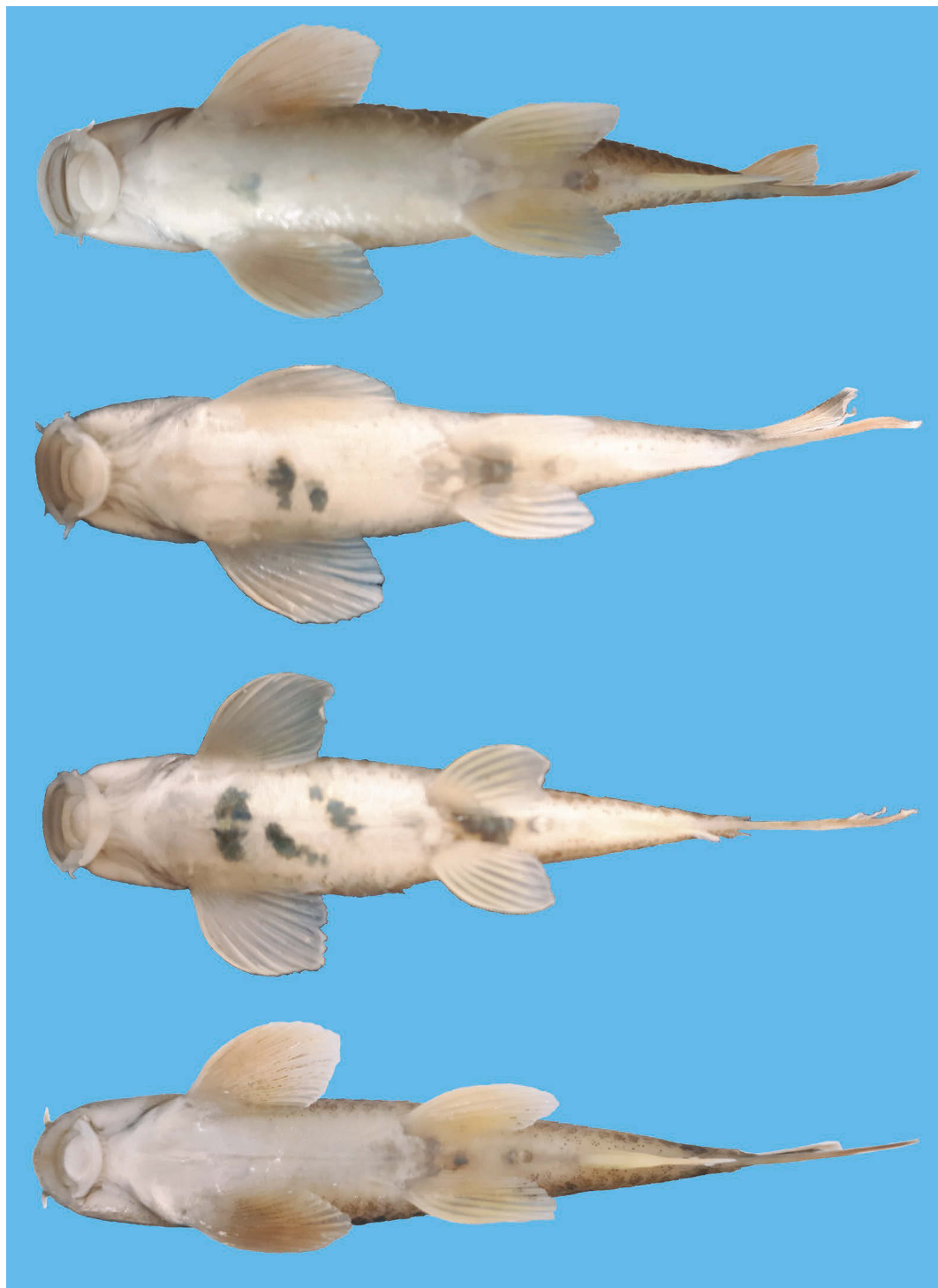


Fig. 12. *Garra tiam*, from top to bottom, IUT-IM T43, holotype, 62.8 mm SL; IUT-IM 13981018-01-01, paratypes, 44.7 mm SL, 54.2 mm SL, 68.1 mm SL; Iran: Abshur River.

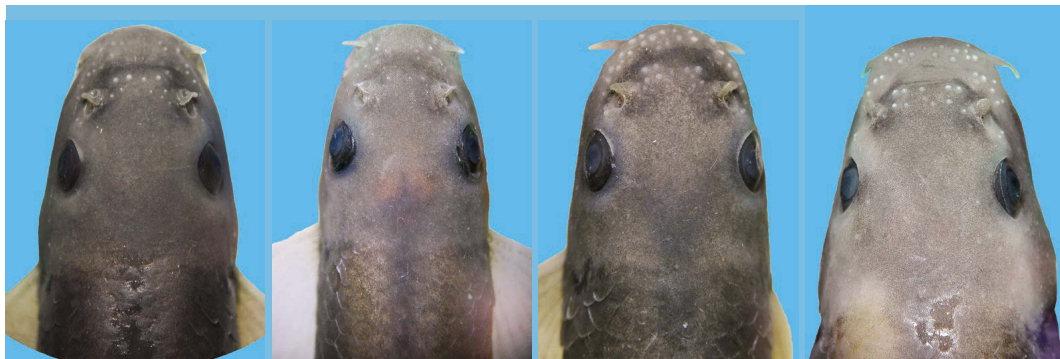


Fig. 13. *Garra tiam*, from left to right, IUT-IM T43, holotype, 62.8 mm SL, IUT-IM 13981018-01-01, paratypes, 44.7 mm SL, 54.2 mm SL, 68.1 mm SL; Iran: Abshur tributary, Karun River.



Fig. 14. *Garra tiam*, from left to right, IUT-IM T43, holotype, 62.8 mm SL; IUT-IM 13981018-01-01, paratypes, 44.7 mm SL, 54.2 mm SL, 68.1 mm SL; Iran: Abshur River.

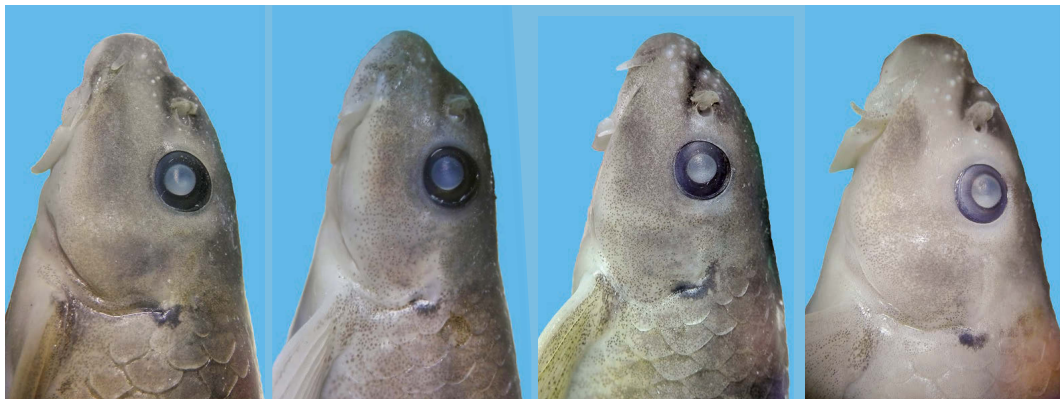


Fig. 15. *Garra tiam*, from left to right, IUT-IM T43, holotype, 62.8 mm SL; IUT-IM 13981018-01-01, paratypes, 44.7 mm SL, 54.2 mm SL, 68.1 mm SL; Iran: Abshur River.



Fig. 16. *Garra tiam*, live coloration, IUT-IM 13981018-01-01, paratype, 70.8 mm SL; Iran: Abshur River.

peduncle, very conspicuous in most specimens, faded in a few. A black or dark-brown blotch at anteriormost lateral line. Pectoral, pelvic and anal fins yellow to dark brown. Some black to dark brown blotches on caudal-fin membranes. Dorsal-fin membranes with a black or dark grey blotch at base, some black or brown blotches on middle and distal dorsal-fin membranes. Iris black. Upper surface of rostral barbel grey.

In life: background colour grey to brown. Fins hyaline; pectoral and pelvic fins golden yellow with black dots; dorsal caudal and anal fins with black blotches. Head grey to green. Iris orange; dark brown spot on upper and lower portions. Scales on flank greenish brown and dark grey, whitish or pale grey on ventral flank and belly. Upper surface of rostral barbel pale grey.

Distribution. *Garra tiam* is currently known from the Abshur, a tributary of the upper Karun River, Tigris River drainage. Abshur River is located in Khozestan Province of Iran, with a length of 70 km. The Abshur River is a perennial river. After crossing from Masjed Suleiman and then Shushtar cities, this river flows into the Karun River.

Etymology. The specific name *tiam* is derived from the word *tiam*, used to refer to someone with beautiful eyes in the language of Lurish people in western Iran, including area of the Abshur River. A name in apposition.

Discussion

Berg (1949) described some *Garra rufa* populations from the Karun River drainage as a subspecies, *G. rufa gymnothorax*, distinguishing from “typical” *G. rufa* by the squamation pattern of the chest and belly which are scaleless in *G. r. gymnothorax* (vs. scaled in *G. r. rufa*). Sayyadzadeh et al. (2015), based on molecular evidence, identified fishes from the Karun River as *G. cf. gymnothorax*, as they were recovered as a distinct lineage from that of *G. rufa*. Esmaeili et al. (2016: 84) referred to these fishes as *G. gymnothorax* and distinguished from *G. rufa* by having a naked chest. We examined specimens of *G. gymnothorax* and *G. rufa* from the Tigris drainage including the Karun (Beshar, Khersan, Bala and Abshur rivers), the Karkheh (Kashkan, Gamasiab and Gharehsoo rivers), as well as Sirvan, Kangir, Godarkhosh, Konjancham, Changuleh and Meymeh rivers. We found that only the specimens from Bala and Abshur rivers (both tributaries of the Karun) exhibit a scaleless chest and belly. Moreover, the squamation pattern of the chest and belly is quite variable in different populations of *G. gymnothorax* and *G. rufa* and therefore it does not allow distinguishing both species. However, our results supported the recognition of most populations of *Garra* from Karun and Karkheh drainages as a clade, for which the name *G. gymnothorax* is available. *Garra gymnothorax* might be indeed a cryptic species and additional research is recommended in order to check for morphological characters to distinguish this species from *G. rufa*.

**Key to species of the *Garra* species
known from the Tigris River drainage
and coastal rivers of Iran**

- 1 – Subterranean species, body whitish or pink; eye absent. 2
– Epigeal species, body brown or grey, usually mottled; eye fully developed. 4
- 2 – Mental disc absent. *G. typhlops*
– Mental disc present. 3
- 3 – Scales absent; pores on lateral line present. *G. lorestanensis*
– Few, often isolated scales present on flank; no pores on lateral line. *G. tashanensis*
- 4 – Mental disc fully attached to ventral part of head. *G. elegans*
– Mental disc with free lateral and posterior margins. 5
- 5 – Usually 8+8 branched caudal-fin rays. *G. persica*
– Usually 9+8 branched caudal-fin rays. 6
- 6 – Usually 8½ branched dorsal-fin rays. 7
– Usually 7½ branched dorsal-fin rays. 8
- 7 – 30–33 total lateral line scales; 12–13 circumpeduncular scales. *G. tiam*
– 32–37 total lateral line scales; 13–17 circumpeduncular scales. *G. gymnothorax*/*G. rufa*
- 8 – Predorsal midline scaleless. *G. mondica*
– Predorsal midline always covered by scales, scales embedded in skin in some individuals. 9
- 9 – Predorsal midline always covered by embedded scales; chest and belly with very small, embedded scales. *G. amirhosseini*
– Predorsal midline usually covered by non-embedded exposed scales; chest covered by large embedded scales and scales on belly not embedded in skin. *G. meymehensis*

Comparative material. All from Iran: *Garra amirhosseini*: IUT-IM 96-10-03, 2, 33.1–45.0 mm SL; Ilam Prov.: Godarkhosh River at road from Ilam to Mehran.

G. gymnothorax: IUT-IM 96-24-01, 13, 38–48 mm SL; Chaharmahal Va Bakhtiari Prov.: Khersan River at road from Yasouj to Esfahan. – IUT-IM 96-03-01, 7, 33.2–48.1 mm SL; Kermanshah Prov.: Gamasiab River at road from Biston to Somghorabad. – IUT-IM 96-04-01, 19, 36.0–48.3 mm SL; Kermanshah Prov.: Gharehsoo River at road from Kermanshah to Kamyaran. – IUT-IM 96-14-01, 3, 33.2–39.2 mm SL; Khozestan Prov.: Balarud at road from Andimeshk to Hoseiniyeh. – IUT-IM 96-23-01, 36, 33.0–52.3 mm SL; Kohkeloyeh Va Boyrahmad Prov.: Beshar River at road from Yasouj to Esfahan. – IUT-IM 96-01-01, 12, 36.3–52.1 mm SL; Lorestan Prov.: Kashkan River at road from Khoram Abad to NoorAbad.

G. rufa: IUT-IM 96-05-01, 3, 33.4–38.2 mm SL; Kurdistan Prov.: Sirvan River at road from Sanandaj to Kermanshah. Ilam Prov.: IUT-IM 96-08-01, 19, 33.1–47.4 mm SL; Kangir River at road from Islamabad-e Gharb to Ivan. – IUT-IM 96-10-01, 13, 33.4–47.0 mm SL; Godarkhosh River at road from Ilam to Mehran. – IUT-IM 96-11-01, 16, 32.2–45.2 mm SL; Konjanchem River at road from Ilam to Mehran. – IUT-IM 96-12-01, 33, 30.1–52.3 mm SL; Changuleh (Talkhab) River at road from Mehran to Dehloran.

Material used in the molecular genetic analysis. All from Iran: *Garra amirhosseini*: IUT-IM 96-10-03, Ilam Prov.: Godarkhosh River at road from Ilam to Mehran (GenBank accession number: MN254982–MN254983).

G. gymnothorax: IUT-IM 96-24-01, Chaharmahal Va Bakhtiari Prov.: Khersan River at road from Yasouj to Esfahan (GenBank accession number: MN255020–MN255026). – IUT-IM 96-03-01, Kermanshah Prov.: Gamasiab River at road from Biston to Somghorabad (GenBank accession number: MN255003–MN255006). – IUT-IM 96-04-01, Kermanshah Prov.: Gharehsoo River at road from Kermanshah to Kamyaran (GenBank accession number: MN255007–MN255015). – IUT-IM 96-14-01, Khozestan Prov.: Balarud at road from Andimeshk to Hoseiniyeh (GenBank accession number: MN255016–MN255019). – IUT-IM 96-23-01, Kohkeloyeh va Boyrahmad Prov.: Beshar River at road from Yasouj to Esfahan (GenBank accession number: MN255027–MN255037). – IUT-IM 96-01-01, Lorestan Prov.: Kashkan River at road from Khoram Abad to

NoorAbad (GenBank accession number: MN254996-MN255002).

G. rufa: IUT-IM 96-05-01, Kurdistan Prov.: Sirvan River at road from Sanandaj to Kermanshah (GenBank accession number: MN255050-MN255051). – IUT-IM 96-12-01, Ilam Prov.: Changuleh (Talkhab) River at road from Mehran to Dehloran (GenBank accession number: MN255065-MN255069, MT159908). – IUT-IM 96-10-01, Ilam Prov.: Godarkhosh River at road from Ilam to Mehran (GenBank accession number: MN255056-MN255062). – IUT-IM 96-08-01, Kermanshah Prov.: Kangir River at road from Islamabad Gharb to Ivan (GenBank accession number: MN255052-MN255055). – IUT-IM 96-11-01, Ilam Prov.: Konjanchar River at road from Ilam to Mehran (GenBank accession number: MN255063-MN255064).

Acknowledgments

We are pleased to thank Mohammad Asghari, Hadi Khoshnamvand and Mojtaba Abbasi for helping with fieldwork, Hajar Tabatabaei for helping with laboratory work and Rasoul Khosravy for helping with data analysis and the Isfahan University of Technology and the Chinese Academic of Sciences for the financial support.

Literature cited

- Berg, L. S. 1949. [Freshwater fishes of Iran and adjacent countries]. Trudy Zoologicheskogo Instituta Akademii Nauk SSSR, 8: 783–858 [in Russian].
- Bruford, M. W., O. Hanotte, J. F. Y. Brookfield & T. Burke. 1998. Multilocus and single locus DNA fingerprinting. Pp. 287–336 in: A. R. Hoelzel (ed.), Molecular genetic analysis of populations: a practical approach. Second edition. IRL Press at Oxford University, New York.
- Esmaili, H. R., G. Sayyadzadeh, B. W. Coad & S. Eagderi. 2016. Review of the genus *Garra* Hamilton, 1822 in Iran with description of a new species: a morpho-molecular approach (Teleostei: Cyprinidae). Iranian Journal of Ichthyology, 3: 82–121.
- Esmaili, H. R., G. Sayyadzadeh, S. Eagderi & K. Abbasi. 2018. Checklist of freshwater fishes of Iran. FishTaxa, 3: 1–95.
- Freyhof, J. 2016. Redescription of *Garra elegans* (Günther, 1868), a poorly known species from the Tigris River drainage (Teleostei: Cyprinidae). Zootaxa, 4173: 496–500.
- Hamidan, N. A., M. F. Geiger & J. Freyhof. 2014. *Garra jordanica*, a new species from the Dead Sea basin with remarks on the relationship of *G. ghorensis*, *G. tibanicus* and *G. rufa* (Teleostei: Cyprinidae). Ichthyological Exploration of Freshwaters, 25: 223–236.
- Hashemzadeh Segherloo, I., A. Abdoli, S. Eagderi, H. R. Esmaili, G. Sayyadzadeh, L. Bernatchez, E. Hallerman, M. F. Geiger, M. Özuluğ, J. Laroche & J. Freyhof. 2017. Dressing down: convergent reduction of the mental disc in *Garra* (Teleostei: Cyprinidae) in the Middle East. Hydrobiologia, 785: 47–59.
- Hashemzadeh Segherloo, I., E. Normandeau, L. Benestan, C. Rougeux, G. Coté, J.-S. Moore, N. A. Ghaedrahmati, A. Abdoli & L. Bernatchez. 2018. Genetic and morphological support for possible sympatric origin of fish from subterranean habitats. Scientific Reports, 8: 1–13.
- Hashemzadeh Segherloo, I., L. Bernatchez, K. Golzari-anpour, A. Abdoli, C. R. Primmer & M. Bakhtiary. 2012. Genetic differentiation between two sympatric morphs of the blind Iran cave barb *Iranocypris typhlops*. Journal of Fish Biology, 81: 1747–1753.
- Higgins, D. G. & P. M. Sharp. 1988. Clustal: a package for performing multiple sequence alignment on a microcomputer. Gene, 73: 237–244.
- Kimura, M. 1980. A simple method for estimating evolutionary rates of base substitutions through comparative studies of nucleotide sequences. Journal of Molecular Evolution, 16: 111–120.
- Kirchner, S., L. Kruckenhauser, A. Pichler, K. Borkenhagen & J. Freyhof. 2020. Revision of the *Garra* species of the Hajar Mountains in Oman and the United Arab Emirates with the description of two new species (Teleostei: Cyprinidae). Zootaxa, 4751: 521–545.
- Kottelat, M. & J. Freyhof. 2007. Handbook of European freshwater fishes. Kottelat, Cornol and Freyhof, Berlin, xiv + 646 pp.
- Kumar, S., G. Stecher & K. Tamura. 2016. Mega7: molecular evolutionary genetics analysis version 7.0 for bigger datasets. Molecular Biology and Evolution, 33: 1870–1874.
- Lanfear, R., P. B. Frandsen, A. M. Wright, T. Senfeld & B. Calcott. 2016. PartitionFinder 2: new methods for selecting partitioned models of evolution for molecular and morphological phylogenetic analyses. Molecular Biology and Evolution, 34: 772–773.
- Mousavi-Sabet, H., M. Saemi-Komsari, I. Doadrio & J. Freyhof. 2019. *Garra roseae*, a new species from the Makran region in southern Iran (Teleostei: Cyprinidae). Zootaxa, 4671: 223–239.
- Mousavi-Sabet, H. & S. Eagderi. 2016. *Garra lorestanensis*, a new cave fish from the Tigris River drainage with remarks on the subterranean fishes in Iran (Teleostei: Cyprinidae). FishTaxa, 1: 45–54.
- Mousavi-Sabet, H., S. Vatandoust, Y. Fatemi & S. Eagderi. 2016. Tashan Cave a new cave fish locality for Iran; and *Garra tashanensis*, a new blind species from the Tigris River drainage (Teleostei: Cyprinidae). FishTaxa, 1: 133–148.
- Ronquist, F., M. Teslenko, P. van der Mark, D. L. Ayres, A. Darling, S. Höhna, B. Larget, L. Liu, M. A. Suchard & J. P. Huelsenbeck. 2012. MrBayes 3.2: efficient Bayesian phylogenetic inference and model choice across a large model space. Systematic Biology, 61: 539–542.

- Sayyadzadeh, G., H. R. Esmaeili & J. Freyhof. 2015. *Garra mondica*, a new species from the Mond River drainage with remarks on the genus *Garra* from the Persian Gulf basin in Iran (Teleostei: Cyprinidae). *Zootaxa*, 4048: 75–89.
- Stamatakis, A. 2014. RAxML version 8: a tool for phylogenetic analysis and post-analysis of large phylogenies. *Bioinformatics*, 30: 1312–1313.
- Stiassny, M. L. J. & A. Getahun. 2007. An overview of labeonin relationships and the phylogenetic placement of the Afro-Asian genus *Garra* Hamilton, 1922 (Teleostei: Cyprinidae), with the description of five new species of *Garra* from Ethiopia, and a key to all African species. *Zoological Journal of the Linnean Society*, 150: 41–83.
- Trewavas, E. 1955. A blind fish from Iraq, related to *Garra*. *Annals and Magazine of Natural History*, 8: 551–555.
- Xia, X. 2013. DAMBE5: a comprehensive software package for data analysis in molecular biology and evolution. *Molecular Biology and Evolution*, 30: 1720–1728.
- Xia, X. 2017. DAMBE6: new tools for microbial genomics, phylogenetics and molecular evolution. *Journal of Heredity*, 108: 431–437.
- Zhang, J., P. Kapli, P. Pavlidis & A. Stamatakis. 2013. A general species delimitation method with applications to phylogenetic placements. *Bioinformatics*, 29: 2869–2876.

Received 22 December 2019
Revised 23 July 2020
Accepted 7 November 2020